Faraday Discussions

Accepted Manuscript

This manuscript will be presented and discussed at a forthcoming Faraday Discussion meeting. All delegates can contribute to the discussion which will be included in the final volume.

Register now to attend! Full details of all upcoming meetings: http://rsc.li/fd-upcoming-meetings

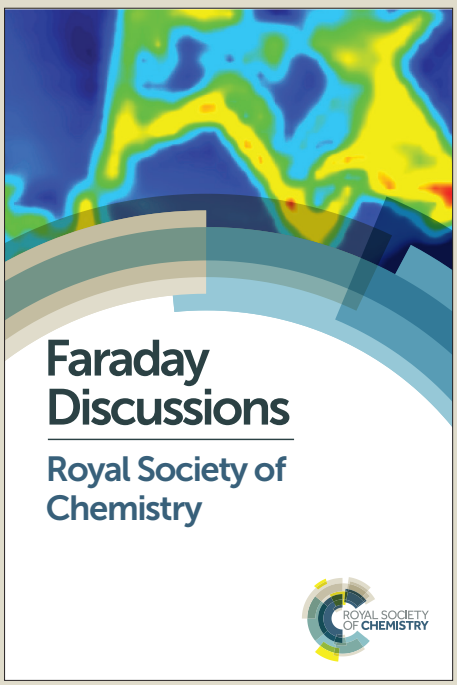

This is an *Accepted Manuscript*, which has been through the Royal Society of Chemistry peer review process and has been accepted for publication.

Accepted Manuscripts are published online shortly after acceptance, before technical editing, formatting and proof reading. Using this free service, authors can make their results available to the community, in citable form, before we publish the edited article. We will replace this *Accepted Manuscript* with the edited and formatted *Advance Article* as soon as it is available.

You can find more information about *Accepted Manuscripts* in the Information for Authors.

Please note that technical editing may introduce minor changes to the text and/or graphics, which may alter content. The journal's standard Terms & Conditions and the Ethical guidelines still apply. In no event shall the Royal Society of Chemistry be held responsible for any errors or omissions in this *Accepted Manuscript* or any consequences arising from the use of any information it contains.

ROYAL SOCIETY OF CHEMISTRY

www.rsc.org/faraday_d

Faraday Discussions

PAPER

Molten salt CO_2 capture and electro-transformation (MSCC-ET) into capacitive carbon at medium temperature: effect of the electrolyte composition

Bowen Deng, Zhigang Chen, Muxing Gao, Yuqiao Song, Kaiyuan Zheng, Juanjuan Tang, Wei Xiao, Xuhui Mao and Dihua Wang*

Received 00th January 20xx, Accepted 00th January 20xx
DOI: 10.1039/x0xx00

Electrochemical transformation of CO_2 into functional materials or fuels (i.e., carbon, CO) in high temperature molten salts have been demonstrated a promising way of CCUS in recent years. In a view of continuous operation, the electrolysis process shall match very well with the CO_2 absorption kinetics. At the same time, in consideration of the energy efficiency, a molten salt electrochemical cell running at lower temperature is more beneficial to a process powered by the fluctuating renewable electricity from solar/wind farms. Ternary carbonates (Li:Na:K=43.5:31.5:25.0) and binary chlorides (Li:K=58.5:41.5), two typical kinds of eutectic melt with low melting point and wide electrochemical potential window, could be the ideal supporting electrolyte for the MSCC-ET process. In this work, the CO_2 absorption behaviour in Li_2O/CaO containing carbonates and chlorides were investigated on a home-made gas absorption testing system. The electrode processes as well as the morphology and properties of carbon obtained in different salts are compared to each other. It was found that the composition of molten salts significantly affect the absorption of CO_2, electrode processes and performances of product. Furthermore, the coupling between the absorption and electro-transformation kinetics are discussed based on the findings.

Introduction

The sustainable increasing of CO_2 concentration in atmosphere has caused great concern for its effect on the change of global climate. In fact, carbon dioxide is not only a greenhouse gas but also an abundant C[1] resource. Therefore, in addition to CO_2 capture and storage (CCS)[1,2], converting CO_2 into useful products such as hydrocarbons and other chemicals is highly desirable for sustainable development.[3,4] Carbon capture, utilisation and storage (CCUS) is very attractive as a mid-term solution owing to relieved burden on limited geological storage sites in CCS process.[5,6] Electrochemical transformation of CO_2 into chemicals, fuels and functional materials, especially driven by renewable electricity is one of the most promising ways of CCUS.

The investigated electrolytes for CO_2 electro-transformation include aqueous solutions[7], ionic liquids[8], high temperature molten salts[9] and solid electrolytes[10]. Electrochemical reduction of CO_2 into low-carbon fuels in aqueous solutions is a proven technology.[11,12] However, the reaction kinetics, current efficiency and the selectivity of products in aqueous solutions is still unsatisfactory due to the poor solubility of CO_2 and limited electrochemical window of the electrolyte, which drives flourishing research of efficient electro-catalysts for CO_2 conversion.[13,14] Ionic liquids are more satisfying candidates due to their low vapour pressure, higher CO_2 absorption capacity and electrochemical stability but the high cost as well as the slow reaction kinetics currently prevent them from massive application.[15,16]

High temperature molten salts are cheaper, abundant and available with high ionic conductivity, low vapour pressure and wide electrochemical window.[17,18] The reaction kinetics can be easily accelerated at elevated temperature without use of complex and costly catalysts [19-23]. Besides, there are plenty of industrial experiences in primary aluminium and magnesium production to scale up the process. Although there is very limited data on the solubility of CO_2 in high temperature molten salts so far, it was recently reported that the absorption capacity of solid absorbent for CO_2 can be activated and improved by molten salts.[24-27] In fact, the absorption of CO_2 in molten salt can be enhanced by a chemical reaction between the acidic CO_2 and alkaline absorbents. Alkali metal oxides and alkali earth metal oxides have strong basicity and would be preferential absorbents. Table 1 presents the equilibrium activity of M_xO (M=Li, Na, K, Ca) under the CO_2 pressure of 1atm at 450 ^oC. All the data is lower than 10^{-4} M, in other words, the equilibrium partial pressure of CO_2 is in the range of 10^{-2} to 10^{-19} atm if the activity of the oxides in the melt could be kept at 0.01 M. From the data in Table 1 and as evidenced by

School of Resource and Environmental Sciences, Hubei International Scientific and Technological Cooperation Base of Sustainable Resource and Energy, Wuhan University, Wuhan 430072, PR China. E-mail: wangdh@whu.edu.cn ; Fax: +86-27-6877-5799; Tel: +86-27-6877-4216

experiments from different groups[9,20,28,29], carbon is the preferential product when Li_2CO_3 and/or $CaCO_3$ is a component of molten salts. Therefore, CO_2 can be absorbed and decomposed in the high temperature molten salts with Li_2CO_3 and/or $CaCO_3$, which forms the fundamental of the molten salt CO_2 capture and electrochemical transformation (MSCC-ET) process.

Table 1 The equilibrium activity of corresponding metal oxide and the deposition potential of metals (E_M) and carbon (E_C) in different molten carbonates at 450 ^oC under CO_2 atmosphere of 1.0 atm.

Molten salt	Activity of M_XO*	E_M/V vs. CO_2-O_2/CO_3^{2-}	E_C/V vs. CO_2-O_2/CO_3^{2-}
Li_2CO_3	1.04×10^{-8}	-3.183	-1.883
Na_2CO_3	2.46×10^{-16}	-2.757	-2.681
K_2CO_3	2.05×10^{-21}	-2.829	-3.251
$CaCO_3$	2.31×10^{-5}	-3.230	-1.523

*The activity of metal carbonate is referred to 1.

The possible products of electrochemical transformation from CO_2 in high temperature molten salts mainly include carbon (in form of carbon powder, film or compounds with metals) and/or carbon monoxide, depending on the temperature and applied cell voltage.[30,31] In some cases, syngas can be obtained when water vapour is present.[32-34] Table 2 briefly summarises the major molten salt systems and the transformation products of MSCC-ET process reported in literature in recent years. The supporting electrolyte (molten salt) can be roughly divided into two categories, molten carbonates and molten chlorides. Usually the melt contains alkaline carbonate or oxide as absorbent, Chen et al recently pointed out that alkaline earth metal oxides/carbonates (CaO, BaO) can also be used as the absorbents for CO_2.[28]

Table 2 CO_2 reduction and obtained product in different molten salt.

Molten salt	Temperature (^oC)	Product	Reference
Li_2CO_3	750-950	CO/carbon	22, 36
Li_2CO_3-K_2CO_3	540-700	carbon nanopowder	19
Li_2CO_3-K_2CO_3	800	Fe_3C	38
Li_2CO_3-Na_2CO_3-K_2CO_3	450-650	carbon powder	20,23,37
$CaCl_2$-CaO	900	carbon	39
LiF-NaF-Na_2CO_3	670-750	carbon particle	40
LiCl-Li_2O	650	carbon	39
LiCl-Li_2CO_3	650	carbon particle	41
LiCl-KCl-K_2CO_3	450	carbon film	21
LiCl-KCl-$CaCl_2$-$CaCO_3$	520	carbon powder	28
NaCl-Na_2CO_3	800	Fe_3C	38

Carbonate melts have been successfully applied in molten carbonate fuel cells (MCFCs) for a long time. It is until recent decade, ternary, binary or single molten alkali carbonates have been applied as the electrolyte for MSCC-ET in the temperature range of 450-950 ^oC as listed in Table 2. In the early of 2000s, Groult et al. synthesised nanostructured carbon by electro-reduction of carbonate anion in fused ternary alkaline carbonates and investigated its potential applications as anode material for lithium ion battery.[20,35] Kaplan et al. reported the

process of converting CO_2 to CO in molten Li_2CO_3 at 850–900 ^oC using a titanium cathode and a graphite anode[36], the reported thermodynamic efficiency exceeded 85%. Licht et al. proposed a solar thermal electrochemical photo (STEP) carbon capture process in molten Li_2CO_3 electrolyte with a nickel cathode and a Pt anode, CO_2 was reduced to CO and C at 750-950 ^oC.[22] Wang et al. reported that CO_2 can be converted into value-added carbon and oxygen using a SnO_2 inert anode in molten Li_2CO_3-Na_2CO_3-K_2CO_3 at 500 ^oC.[23] The influences of temperature and cell voltage on the process were investigated in detail lately.[37] Chen et al. also reported carbon powder by electro-reduction of CO_2 in Li_2CO_3-K_2CO_3 at 500-700 ^oC.[19] More recently, Chery et al. analysed and reviewed that the thermodynamic of the reduction of CO_2 in molten carbonates.[30,31]

As shown in Table 2, the reduction of CO_2 can also be achieved directly or indirectly in carbonate-containing molten halides.[39] Ito and Kawamura reported that carbon film deposited on an aluminium electrode in LiCl-KCl-K_2CO_3 melts when CO_2 was fed into the cell. The current density was 100 mA cm^{-2}, much higher than that reported in aqueous solution.[21] Thermodynamically K_2CO_3 was converted into Li_2CO_3 in the melt for the Gibbs energy change of $2LiCl+K_2CO_3=Li_2CO_3+2KCl$ is -105.31 kJ/mol. Similar works were reported in LiF-NaF-Na_2CO_3 melt and LiCl-Li_2CO_3 melt.[40,41] It is more recently that Chen et al. reported carbon deposition in $CaCl_2$-$CaCO_3$-LiCl-KCl, confirming the possibility of CO_2 capture and reduction from $CaCO_3$-containing molten chlorides.[28] It was also reported that mild steel or titanium can be electro-carburized using CO_2 feedstock in molten carbonate salts to form a hardened surface.[38,42] These studies demonstrated that the electrochemical reduction of carbonate/CO_2 are significantly influenced by electrolysis temperature, cell voltage and melt composition, etc.

The mechanism for the MSCC-ET process can be briefly presented as equations (1) to (4). In the molten salts containing M_xCO_3 (M=Li, Ca, …), the carbonate is reduced to carbon (equation (1) and (2)) or carbon monoxide (equation (1a) and (2a)) with release of metal oxide and oxygen. The difference between equation (1) and (2) is due to the difference of the anodic reaction. Depending on the experimental condition, the formed CO can be further reduced to C (equation (3)). The as-formed oxides can absorb CO_2 to regenerate carbonates (equation (4)), maintaining the sustainable operation of the process. The molten salt suitable for production of carbon from CO_2 should be able to dissolve oxygen ions by which CO_2 can be absorbed and converted to carbonate ions.

$$3M_xCO_3 = 3M_xO + C + 2CO_2 + O_2 \quad (1)$$

$$4M_xCO_3 = 4M_xO + 2CO + 2CO_2 + O_2 \quad (1a)$$

$$M_xCO_3 = M_xO + C + O_2 \quad (2)$$

$$2M_xCO_3 = 2M_xO + 2CO + O_2 \quad (2a)$$

$$2CO = 2C + O_2 \quad (3)$$

$$M_xO + CO_2 = M_xCO_3 \quad (4)$$

If the MSCC-ET process was driven by electricity from fossil fuels, it will generate more CO_2. A desirable process is driven by renewable energy and/or industrial waste heats, therefore, maintaining molten salt bath at relatively low temperature would be more preferential to prevent heat loss and corrosion of structural materials. Furthermore, carbon thermodynamically tends to be the reduction product from CO_2 at lower temperature.[30,31] It is well known that Li_2CO_3-Na_2CO_3-K_2CO_3 (43.5:31.5:25mol%) and LiCl-KCl (58.5:41.5mol%) are typical eutectics with low melting point, 393 ^oC and 353 ^oC, respectively. Besides, they all have wide electrochemical window and are able to dissolve alkaline oxides or carbonates. As shown in Table 2, the reduction products were significantly influenced by the composition of molten salts as well as experimental conditions such as temperature, electrode materials. In fact, due to their different physicochemical properties of molten salts such as basicity, solubility, viscosity and etc., both of CO_2 absorption and electrochemical reaction process would be affected by the molten salt composition. In this work, the absorption kinetics, electrochemical behaviour, energy efficiency, properties of products of the two kinds of low temperature MSCC-ET electrolyte were investigated and compared in detail. Furthermore, the kinetic coupling between the CO_2 absorption and electrochemical transformation was also discussed based on the obtained results.

Experimental

CO_2 absorption

CO_2 absorption studies were carried out by a home-made gas absorption experimental set-up. The set-up was consisted of two high temperature vessels (a gas storage vessel and a CO_2 absorption vessel, interconnected by a valve) with identical volume (3.5 L). An alumna

crucible with 100 g salts (typically, 180 mmol/kg Li_2O-containing molten Li-Na-K carbonates or 180 mmol/kg Li_2O/CaO-containing molten Li-K chlorides) was placed on the bottom of the absorption vessel. Before absorption, the connected vessels were purged with argon and evacuated to nearly vacuum repeatedly at room temperature, and then they were separated to each other by turning off the valve. The set-up was then heated up to 450 ^{o}C at a rate of 5 ^{o}C/min. Certain amount of CO_2 gas (99% purity) was purged into the gas storage vessel after temperature was stable. After equibrium, CO_2 was introduced into the absorption vessel by turning on the valve quickly. The internal pressure and temperature was automatically monitored by a digital pressure indicator with a precision of ±0.001 kPa and a thermal couple with accuracy of ±0.01 K, respectively, which were recorded and stored in a personal computer. All trials were carried out for at least 3 times, and a mean value was reported here. The absorption amount of CO_2 was calculated according to the transient pressure of the reactor:

$$n_{CO_2} = \frac{P_g V_g - P(V_g + V_e - V_m) + P_v V_m}{RT} \quad (5)$$

Where n_{CO_2} (mmol) is the absorption amount of CO_2 at given time t (min), P_g (kPa) is the initial CO_2 pressure in gas storage vessel, P (kPa) is the CO_2 pressure at time t (min), and P_v (kPa) is the saturated vapour pressure of eutectic melts. V_g (cm^3) and V_e (cm^3) are the volume of the gas storage and the absorption vessel, respectively. V_m (cm^3) and V_c (cm^3) represent the volume of molten salts and crucible, respectively.

Cyclic voltammetry and electrolysis

Cyclic voltammetry was applied to investigate the electrochemical behaviour of the eutectic melt with different composition under CO_2 atmosphere. Molten Li-Na-K carbonates (43.5:31.5:25 mol%) or molten Li-K chlorides (58.5:41.5 mol%) with 2 mol% Li_2CO_3/$CaCO_3$ were used as the electrolytes. Approximately 500 g salt was dried at 250 ^{o}C under argon for up to 24 h to remove original moisture before it was heated up to the desired temperatures under CO_2. CO_2 was continuously bubbled into the melt through an alumina tube during the tests. CV measurements were performed on an electrochemical workstation (CHI-1140, CH Instrument Co. Ltd., USA) using a three-electrode configuration. The reference electrode constituted of a silver wire placed in an alumina tube filled with 0.5 mol% Ag_2SO_4-containing molten Li_2CO_3-Na_2CO_3-K_2CO_3 or 0.5 mol% AgCl-containing LiCl-KCl respectively. The working and counter electrode were a nickel (Ni) wire (1 mm in dia., 0.64 cm^2 in electrolyte) and a graphite rod (6mm in dia., 4.00 cm^2 in electrolyte), respectively.

Galvanostatic electrolysis at a current density of 25 to 100 mA cm^{-2} was carried out in defferent melts using a computer-controlled power source (Shenzhen Neware Electronic Co. Ltd., China). A Ni sheet (24 cm^2 area) and graphite rod (44 cm^2 area) were served as cathode and anode, respectively. CO_2 was bubbled into the melts during electrolysis. Products deposited on the cathode were collected and rinsed with 1 M HCl and distilled water to remove the adherent frozen electrolyte, and were dried in a vacuum oven at 80 ^{o}C for 12 hours.

Characterization and electrochemical performance of the obtained carbon

The obtained products were characterized by scanning electron microscopy (SEM, FEI Sirion field emission), X-ray diffraction spectroscopy (XRD, Shimadzu X-ray 6000 with Cu Kα radiation at 40 kV and 250 mA, λ=0.154 nm), Laser Confocal Raman Microspectroscopy (Renishaw RM1000, UK) at room temperature with an excitation wavelength at 514.5 nm from a diode pumped solid-state laser and a Micromeritics ASAP 2020 automatic analyser at liquid N_2 temperature.

The capacitive performance of carbon samples was investigated in 6 M KOH with a two-electrode testing cell. The electrodes were prepared into carbon films by mixing the carbon with polytetrafluoroethylene (PTFE) and commercial acetylene black (8:1:1). Nickle foam was used as current collector and was covered by the carbon film with a surface area of about 0.8 cm^2. The mass loading of the active material was approximately 5 mg cm^{-2}. Two electrodes with almost identical mass loading were assembled in a cell for the measurements. Their capacitive performances were evaluated by cyclic voltammetry and galvanostatic charge–discharge measurements, which were carried out on a PGSTAT 302N Autolab Electrochemical Workstation. The gravimetric capacitances Cg (F/g) were then calculated from the measured capacitance and the mass of active material.

Results and discussion

The static absorption curves of CO_2 by different molten salts at 450 ^{o}C under the CO_2 partial pressure of 50 kPa are shown in Fig. 1. As can be seen, absorption of CO2 in blank molten LiCl-KCl is negligible, while CO_2 solubility in oxide-free molten ternary carbonates was much higher, approximately 6 mmol CO_2 was absorbed by 100 g blank Li-Na-K carbonates. The results demonstrated that the structure and

composition of molten salts has significant effect on the CO_2 absorption. Molten carbonates have stronger interaction with CO_2 than molten chlorides. The following chemical capture mechanism[43,44] (eqs. 6 and 7) could be possible for molten carbonates.

$$CO_2 + CO_3^{2-} = C_2O_5^{2-} \quad (6)$$

$$CO_2 + nCO_3^{2-} = C_{n+1}O_{3n+2}^{2-} \quad (7)$$

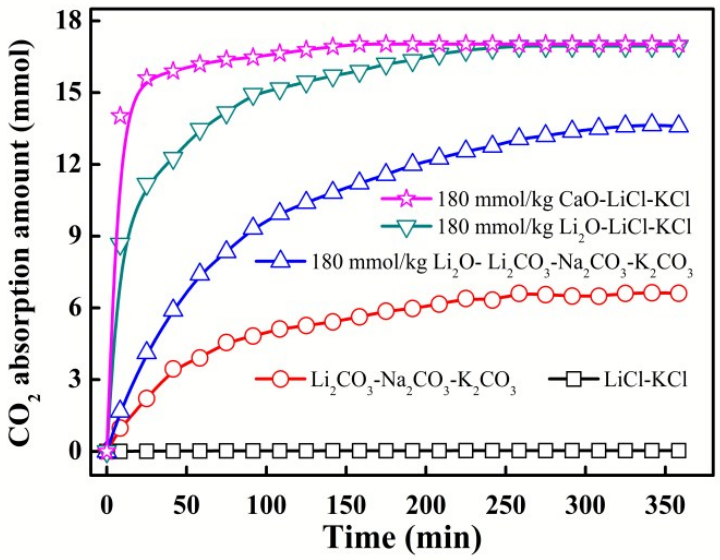

Fig. 1 CO_2 absorption curves in different salts (100 g) at 450 °C under the CO_2 partial pressure of 50 kPa.

Interestingly, very different absorption behaviours present when 18 mmol Li_2O or CaO was added into 100 g salts, respectively. CO_2 can be rapidly captured when Li_2O or CaO was added into molten LiCl-KCl. The LiCl-KCl melt with CaO and Li_2O absorbed 17 mmol and 16.9 mmol CO_2, respectively when the equilibrium was reached. According to the absorption reaction as shown in equation (4), the conversion efficiency is around 94% for Li_2O and CaO in the molten chlorides. Besides, it took less time to reach absorption equilibrium in molten chlorides than in molten carbonates with CaO or Li_2O, totally different from the blank molten salts. The absorption kinetics of CaO in moten chlorides is much faster and reached equilibrium within 2 hours although its absorption equilibrium constant is much lower than that of Li_2O. The conversion efficiency of Li_2O in molten carbonate (approximately 45%) is much lower than that in molten chlorides (approximately 94%), suggesting the property of molten salt affect both of the absorption thermodynamic and kinetics of Li_2O. This phenomenon might be due to the lower activity of Li_2O in the molten ternary carbonates and the stronger interaction between CO_2 and carbonate slow down the diffusion rate of CO_2 in the melt. It seems that CaO was a stronger absorbent for CO_2 in molten LiCl-KCl due to its faster absorption rate and higher conversion efficiency. The experimental results demonstrated that Li_2O and CaO can serve as a good absorbent in molten salts so that it can be acted as a shuttle to maintain MSCC-ET process given by eqs. (1) to (4). It should be pointed out that the absorption behaviour of CO_2 is affected by its partial pressure, temperature and the concentration of Li_2O/CaO as well as the composition of molten salts. And the curve as shown in Fig. 1 is a boundary condition for no forced convention is involved.

To evaluate the electrochemical transformation behaviour of the captured CO_2 (in the form of carbonate), cyclic voltammetry measurements were conducted in molten Li_2CO_3-Na_2CO_3-K_2CO_3, 2 mol% Li_2CO_3-LiCl-KCl and 2 mol% $CaCO_3$-LiCl-KCl under CO_2 atmosphere at 450 °C with a Ni wire working electrode. As shown in Fig. 2, there are obvious reduction peaks before the deposition of alkali metal in the three kinds of electrolyte, suggesting the reduction of carbonate anion can take place before the decomposition of electrolyte. However, there exists some difference on the CV curves obtained in the three molten salts. From Fig. 2a, there is only one reduction peak at -2.1 V (vs. Ag^+/Ag) before the cathodic limit in molten Li-Na-K carbonates, which could be ascribed to the reduction of CO_3^{2-} to carbon with 4-electron transfer, as presented by eqs. (1) and (2). However, there are two reduction peaks before the deposition of alkaline metals on the CVs in molten LiCl-KCl containing Li_2CO_3 as shown in Fig. 2b. The reduction of carbonate/CO_2 in molten LiCl-KCl containing 2 mol% Li_2CO_3 occurred in the potential range from -1.2 to -2.2 V (vs. Ag^+/Ag). Two reduction peaks were presented at -1.5 V and -1.9 V,

respectively. The two-step electrochemical reduction might be caused by a quasi-reversible reduction of CO_2 to a CO_2^{2-} radical (eqs. 8) and followed by the reduction of chemically as-formed CO (eqs. 9) to carbon (eqs. 10).[9,30] Also, it was reported that carbonate ions can be reduced in another two steps as represented by eqs. (12) and (13),[9] firstly reduced to CO_2^{2-}, and CO_2^{2-} was then reduced to carbon.

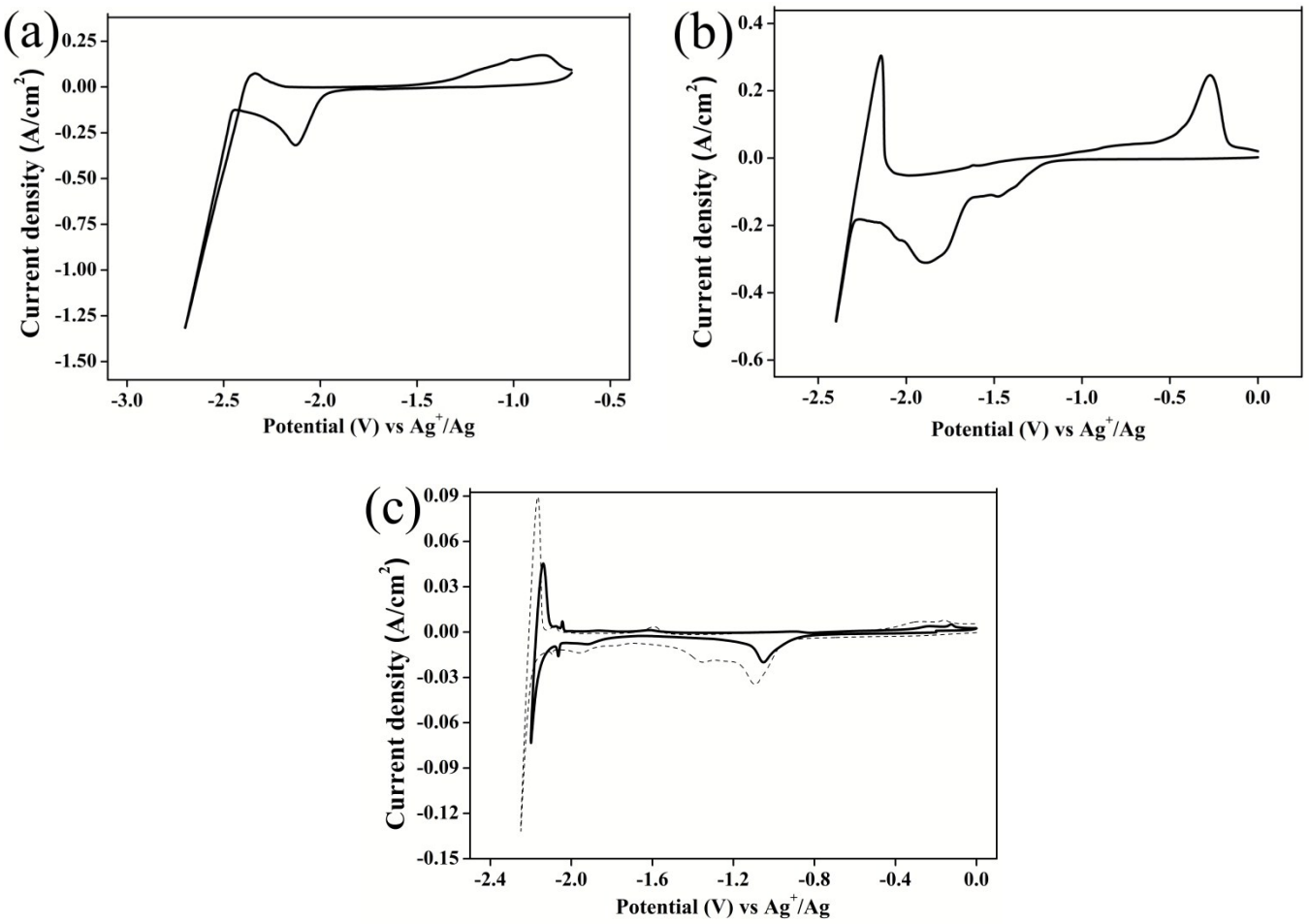

Fig. 2 Cyclic voltammograms of nickel wire electrode in (a) Li_2CO_3-Na_2CO_3-K_2CO_3 (b) 2 mol% Li_2CO_3-LiCl-KCl (c) 2 mol% $CaCO_3$-LiCl-KCl under 1.0 atm CO_2 atmosphere at 450 °C. Solid line: cyclic voltammetry conducted in original molten mixture. Dashed line: cyclic voltammetry conducted after potentiostatic eletrolysis at -2.2 V.

First step: quasi reversible reduction: $CO_2 + 2e^- = CO_2^{2-}$ (8)

Second step: chemical formation of CO: $CO_2^{2-} = CO + O^{2-}$ (9)

Third step: irreversible electro-reduction of CO to carbon: $CO + 2e^- = C + O^{2-}$ (10)

Overall reaction: $3CO_2 + 4e^- = C + 2CO_3^{2-}$ (11)

$CO_3^{2-} + 2e^- = CO_2^{2-} + O^{2-}$ (12)

$CO_2^{2-} + 2e^- = C + 2O^{2-}$ (13)

In the salt of 2 mol% $CaCO_3$-LiCl-KCl, different CV profile was recorded for the first cycle as shown as the solid line in Fig. 2c. There is only one reduction peak in the potential range of -1.2 V to -0.8 V, and no carbon deposit was found by potentiostatic electrolysis using a nickel sheet electrode in the potential range. It is likely that the reduction peak is related to the reduction of the carbonate ion to CO on nickel electrode in the melt. It is different from that in Li_2CO_3 containing chloride melt, and also different from that in $CaCO_3$-$CaCl_2$-LiCl-KCl melt with high $CaCO_3$ concentration in which one-step reduction to carbon was proposed[28]. However, carbon deposit was obtained by electrolysis at more negative potential (-2.2 V) in the melt. More interestingly, after that, similar two reduction peaks were found in 2 mol% $CaCO_3$-LiCl-KCl (dashed line in Fig. 2c), the reduction peaks at -1.1 V and -1.4 V, respectively were more positive than that of Li_2CO_3 reduction. And then carbon deposit was found under potentiostatic electrolysis of -1.8 V. The possible reason might be the partial transformation of $CaCO_3$ to Li_2CO_3 under the electrolysis condition, as the standard equilibrium constant for the reaction of $2LiCl(l)+CaCO_3(l)=CaCl_2(l)+Li_2CO_3(l)$ is only 2.97×10^{-3} at the temperature. The different CV behaviours demonstrate that the reduction of carbonate ion was very sensitive to the composition of molten salts as well as electrode materials, which remains more investigation. Besides, it should be noted that a weak anodic peak was found at -0.3 V (vs. Ag^+/Ag), which can be ascribed to the oxidation of deposited carbon on Ni wire working electrode by eqs. (14) and/or eqs. (15). By contrast, more intensive oxidation peaks were found in Li_2CO_3-containing molten salt as presented on Fig. 2a and Fig. 2b. This difference might be caused by poorer adherence for the deposited carbon and stronger evolution of formed CO in $CaCO_3$-containing LiCl-KCl.

$$C + 2CO_3^{2-} = 3CO_2 + 4e^- \quad (14)$$

$$C + 2O^{2-} = CO_2 + 4e^- \quad (15)$$

Galvanostatic electrolysis was carried out in the three kinds of melts at current density range from 25 mA cm^{-2} to 100 mA cm^{-2} by passing passing same amount of electrical charge (2000 mAh). The cell voltage-time plots were recorded and displayed in Fig. 3. As can be seen, cell voltage in Li_2CO_3-Na_2CO_3-K_2CO_3 was much lower than that in molten chlorides at either 25 mA cm^{-2} or 100 mA cm^{-2}. The cell voltage for carbon deposition at 25 mA cm^{-2} was in the vicinity of 2.6 V for molten carbonates while that was nearly 3.2 V in carbonate-containing chlorides. It is noted that the cell voltage in $CaCO_3$ containing system is slightly lower than that in Li_2CO_3 containing chloride. When the current density was increased to 100 mA cm^{-2}, the voltage-time profile is quite different in the three salts as shown in Fig. 3b. The cell voltage in the ternary carbonates was low and gradually decreased with time, probably due to the decreasing of real current density on the cathode. While the cell voltage in carbonate containing chlorides showed a profile of sharply increasing followed by gradual increase and then reaching stability. These might be partially due to the concentration polarization of carbonate ion on the electrodes. It is noted that the cell voltage in $CaCO_3$ containing salt is 200-300 mV higher than that in Li_2CO_3-containing chlorides, due to the more complicated and sluggish reduction kinetics in the $CaCO_3$ containing melt, in consistent with its CV behaviour as shown in Fig. 2. The lowest cell voltage for CO_2 reduction in Li-Na-K molten carbonates is beneficial to decrease the energy consumption of the process.

Current efficiency at different current density in the melts was calculated based on the mass of the carbon product and depicted in Fig. 4. As can be seen, highest current efficiency of approximately 90% was obtained in the ternary carbonate melt, and the current efficiency decreased with increasing current density. Current efficiency in Li_2CO_3 containing chlorides is higher than that in chlorides with $CaCO_3$. The efficiency is higher than 65% in all experimental conditions, which demonstrated that carbon is the preferential reduction product at the temperature in all electrolytes. Combing with the data of cell voltage and current efficiency, the energy consumption for electrolytic reduction of CO_2 to carbon in ternary carbonates is the lowest.

The SEM images of carbon deposited in various molten salts at same current density (50 mA cm^{-2}) are shown in Fig. 5. As can be seen, carbon obtained in molten Li-Na-K carbonates consisted of highly aggregated nanoparticles in a size of 50 nm to 100 nm. While the morphology of carbon deposited in 2 mol% Li_2CO_3-LiCl-KCl was quite complex, including nanoparticles, quasi-spherical carbon as well as micron-size carbon sheet. Likewise, similar morphology of the deposited carbon was found in 2 mol% $CaCO_3$-LiCl-KCl, which is mainly constituted of micron-size carbon sheet and shell-like carbon, and a small quantity of nanoparticles was also observed. It is interesting that the morphology of deposited carbon is significantly influenced by the composition of molten salts. The results inferred that the appearance of micron-size carbon sheet is relevant to Li-K chlorides and electrolysis temperature, since no carbon sheet was found in molten LiCl-Li_2CO_3 at 650 ^oC [41]. However, carbon particles with much smaller size were obtained in Li2CO3-Na2CO3-K2CO3, which might be ascribed to much higher concentration of Li2CO3 in the ternary carbonates, comparing with the quasi-spherical carbon in a size of 500-800nm obtained in Li2CO3-containing molten halides [41,45]. Possibly due to the template effect of chloride salts, carbon sheets were obtained in the melts at the experimental temperature. While the shell-like morphology observed in CaCO3 containing chlorides might be related to its special reduction mechanism, i.e., CO as an intermediate product.

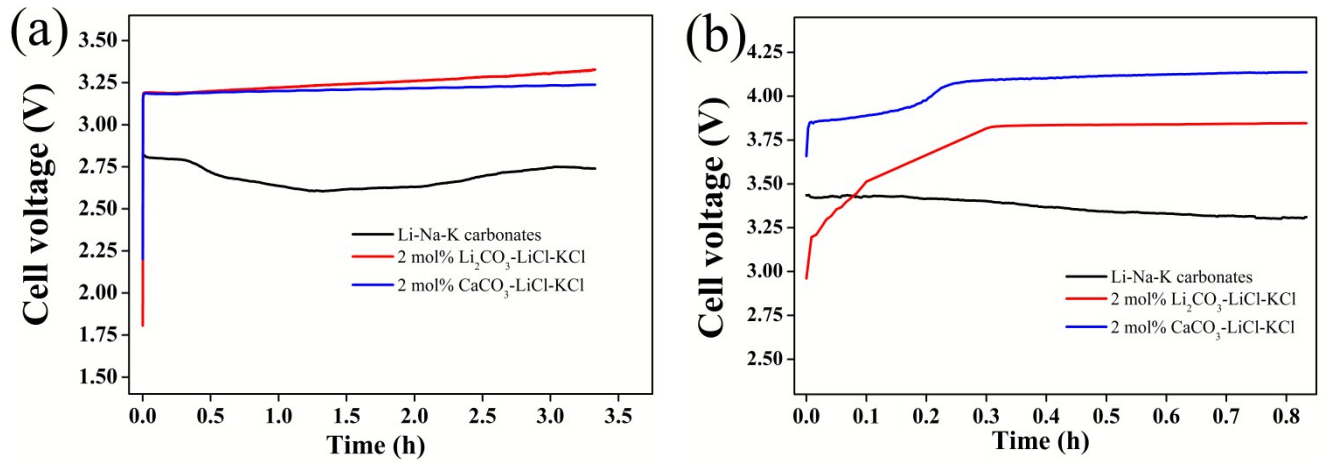

Fig. 3 The voltage-time plots for galvanostatic electrolysis in different molten salt at various current densities under CO_2 atmosphere at 450 ^{o}C with charge of 2000 mAh. (a) 25 mA cm^{-2} .(b) 100 mA cm^{-2}.

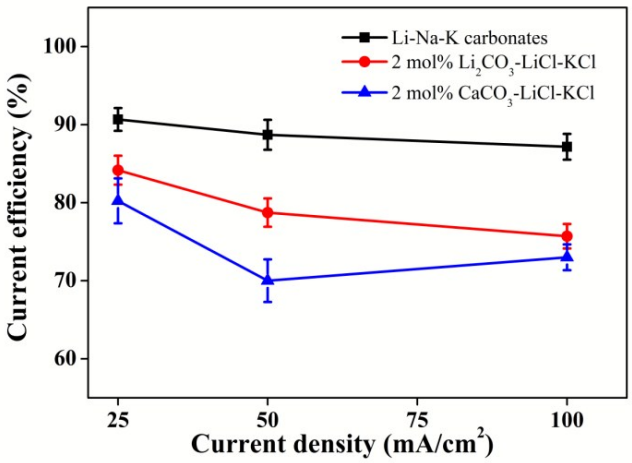

Fig. 4 Current efficiency for galvanostatic electrolysis in different molten salt under CO_2 atmosphere at 450 ^{o}C with total charge of 2000 mAh.

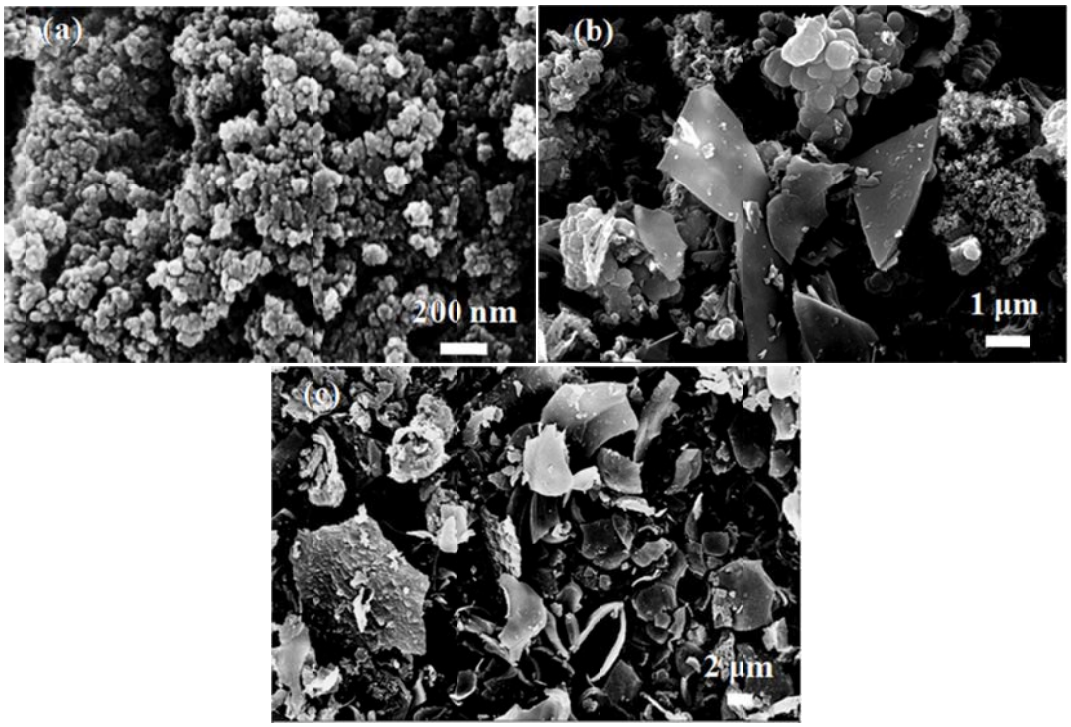

Fig. 5 The morphology of carbon deposited at 50 mA cm^{-2} in various molten salt under CO_2 atmosphere at 450 °C. (a) Li_2CO_3-Na_2CO_3-K_2CO_3 . (b) 2 mol% Li_2CO_3-LiCl-KCl. (c) 2 mol% $CaCO_3$-LiCl-KCl.

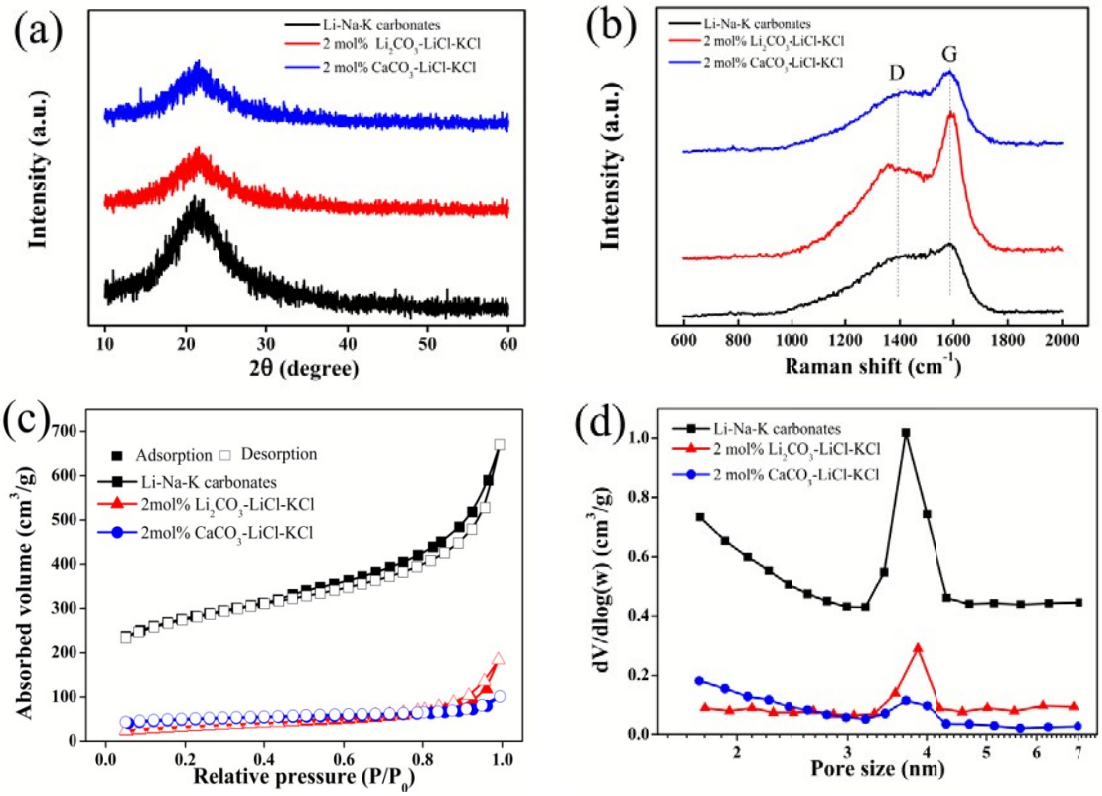

Fig. 6 Characterization of carbon obtained in various molten salts at 50 mA cm^{-2} under CO_2 atmosphere at 450 °C (a) XRD. (b) Raman spectrum. (c) nitrogen adsorption-desorption isotherm. (d) pore size distribution.

The deposited carbon at 50 mA cm^{-2} in various molten salts was further studied by XRD as shown in Fig. 6a. They are amorphous as reported elsewhere[23,37] since no obvious diffraction peak was found. Fig. 6b displays the Raman spectra of the carbon obtained in different salts. Two bands located at 1395 and 1592 cm^{-1} represent the characteristic disordered (D) and graphitic (G) planes of carbon material, respectively. The lower D band peak suggests the appearance of a low degree of structure defects in the carbon material. The ratio of intensity of D and G bands (I_D/I_G) for the carbon obtained in the three melts are shown in Table 3. It is around 0.7 for the carbon obtained from molten chlorides, but it is 0.86 for the carbon from the ternary carbonates. The low I_D/I_G indicates the relatively high degree graphitic structure in the as-prepared carbon in molten chlorides, this is related to the existence of carbon sheets as found in products obtained in carbonate-containing LiCl-KCl. While there are more defects in the carbon obtained from molten carbonates under the experimental condition, suggesting a highly activate surface carbon with large amount of defects. The specific area and the porosity information of the products were further measured by N_2 adsorption-desorption automatic analyser and calculated by the Brunauer-Emmett-Teller (BET) method and the Barret-Joyner-Halender (BJH) method, respectively. The results are shown in Fig. 6c, 6d and Table 3. The porosity and the specific surface area of carbon deposited in Li-Na-K carbonates is much larger than that of carbon obtained in carbonate-containing LiCl-KCl. The BET area of carbon from molten carbonates is 897.4 $m^2\ g^{-1}$, much higher than that from molten chlorides (113.9 and 157.9 $m^2\ g^{-1}$, respectively). Also, its pore volume is much larger.

Table 3 Characterisation summary of Raman and nitrogen adsorption-desorption tests for carbon deposited at 50 mA cm^{-2} in different molten salt.

Molten salt	I_D:I_G	S_{BET} ($m^2\ g^{-1}$)	Pore volume ($cm^3\ g^{-1}$)	Average pore size (nm)
Li_2CO_3-Na_2CO_3-K_2CO_3	0.86	897.4	0.862	4.62
2 mol% Li_2CO_3-LiCl-KCl	0.67	113.9	0.279	9.97
2 mol% $CaCO_3$-LiCl-KCl	0.72	157.9	0.125	3.98

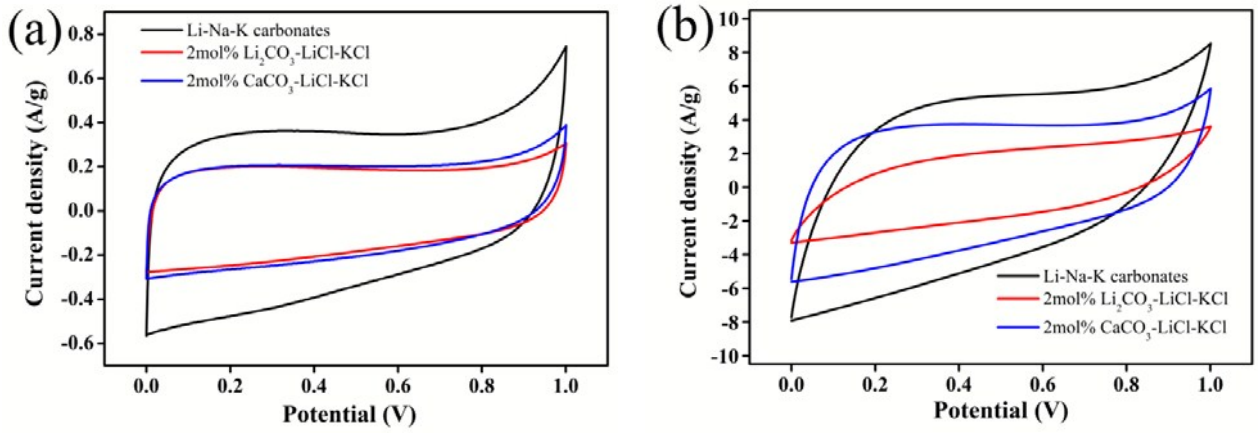

Fig. 7 Cyclic voltamograms of the carbon obtained at 50 mA cm^{-2} in various molten salts at 450 °C as working electrode in 6 M KOH aqueous solution under different scan rate. (a) 5mV/s. (b) 100 mV/s.

Fig. 7 and Fig. 8 present the electrochemical performances of the carbon obtained in different molten salts investigated by cyclic voltammetry and galvanostatic charge-discharge tests, respectively using a carbon film electrode. As shown in Fig. 7a and Fig. 7b, CV plots for carbon obtained in Li-Na-K molten carbonates and CaCO3-containing LiCl-KCl were more rectangular, and corresponding current density of plateaus were larger than those of carbon deposited in Li2CO3-containing LiCl-KCl. Accordingly, the results of galvanostatic charge-discharge also demonstrate that a promising capacitive properties of carbon obtained in Li-Na-K molten carbonates with 240 F/g at current density of 0.2 A/g, while capacitance for carbon deposited in 2 mol% Li2CO3-LiCl-KCl and 2 mol% CaCO3-LiCl-KCl were 102 F/g and 145 F/g at 0.2 A/g, respectively (Fig. 8a). And the result of capacitance obtained at 2 A/g of charge-discharge current density was 202 F/g, 71 F/g and 110 F/g respectively as presented in Fig. 8b. This result suggests better electrochemical performance of deposition carbon can be obtained in Li-Na-K molten carbonates attributed to its higher surface area and porosity. Capacitive property of carbon obtained in CaCO3-

containing LiCl-KCl seems to be more attractive than carbon deposited in Li2CO3-containing LiCl-KCl due to its higher surface area as shown on Table 3. Different morphology, structure and electrochemical performance for carbon obtained in molten salts with different composition may suggest a different application field for the relative products.

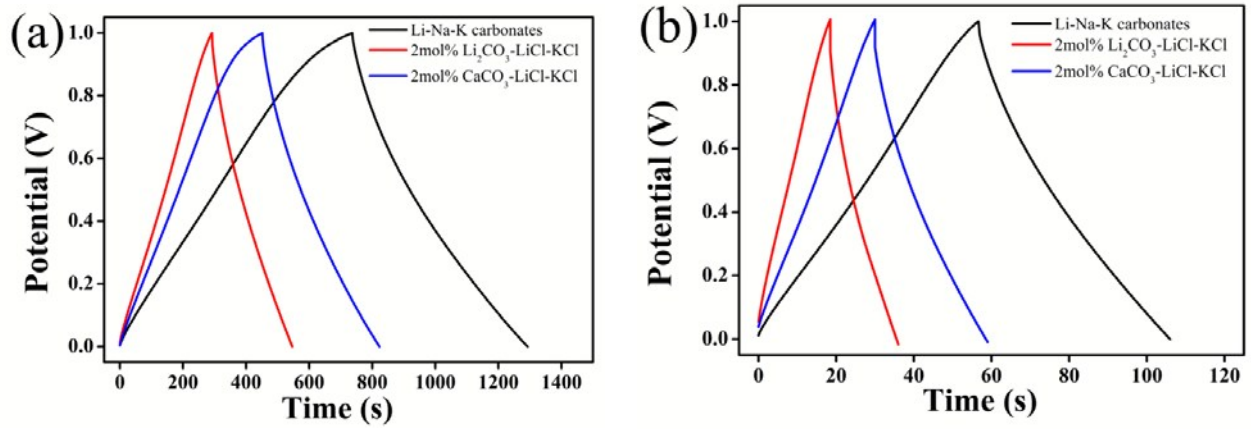

Fig. 8 Charge-discharge curves for carbon obtained at 50 mA cm^{-2} in various eutectics. (a) charge-discharge at 0.2 A/g. (b) charge-discharge at 2 A/g.

Prospects

For the continuous operation of MSCC-ET process, it is expected that the kinetics of CO2 absorption, the diffusion of carbonate ion should be well matching with the electrochemical kinetics on the electrodes, just like industrial production of primary aluminium in which the dissolution of alumina shall be well coupled with the electrode kinetics. Therefore, based on the absorption curve of CO_2 as shown in Fig. 1, CO_2 transportation rate in molten salt was calculated and analysed according to Damping-Film Theory[46]. The relationship between absorbed CO_2 and absorption time can be stated as follows:

$$\ln[(n_e - n)/n_e] = -Kt \tag{16}$$

Where n_e (mmol) denotes the uptake amount at absorption equilibrium and n (mmol) is the mole of absorbed CO_2 at any time, which can be calculated by eqs. (5). And K represents the reaction rate constant.

Fig. 9 shows the absorption rate of CO_2 calculated by eqs. (16) based on the data in Fig. 1. The slope of each curve represents the instant absorption rate of the melt. As can be seen, absorption rate of CO_2 in CaO-containing LiCl-KCl was the fastest. Also it can be found that the curves in the three molten salts were pseudo-linear within the initial 300 seconds, suggesting a constant uptake rate during the first 5 minutes. Thus the apparent absorption rate of CO_2 capture can be calculated by eqs. (17) according to the results of CO_2 absorption kinetics. The optimum coupling electrolysis is assumed when the electrochemically regeneration rate of oxygen ions (eqs. 18) equals to the consumption rate of oxygen ions by CO_2 absorption (eqs. 20). Following this idea, the suitable current density for electrolysis with 100% efficiency can be calculated by eqs. (21) according a 4-electron transfer mechanism as shown by eqs. (18).

$$v_{CC} = \frac{dn}{dt} = \frac{n_{CO_2}}{\frac{m}{M}\cdot t} \tag{17}$$

n (mmol) ------ absorbed amount of CO_2 *m (g) ------the weight of molten mixture*

M (g mol^{-1}) ------ the molar weight of molten mixture *t (h)------ peseudo-linear absorption time*

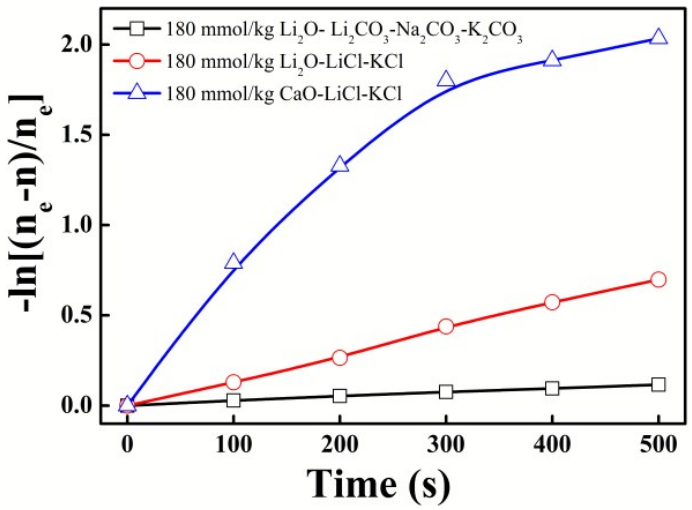

Fig. 9 CO_2 absorption rate in various molten salts under 50 kPa CO_2 partial pressure at 450 °C.

Table 4 The optimum coupling kinetics between a static CO_2 absorption and electrolysis under 50 kPa CO_2 partial pressure and at 450 °C in different molten salts.

Molten salt composition	Molar amount of molten mixture (g mol^{-1})	CO_2 absorption rate ($mmol_{CO_2}$ h^{-1} mol_{salt}^{-1})	Coupling electrolysis rate (mA cm^{-2} mol_{salt}^{-1})
180 mmol/kg Li_2O Li-Na-K molten carbonates	100.1	12.0	53.6
180 mmol/kg Li_2O LiCl-KCl	56.0	33.7	150.5
180 mmol/kg CaO LiCl-KCl	56.2	53.6	239.5

$$CO_3^{2-} + 4e^- = C + O^{2-}(regeneration) + 2O^{2-}(anodic-oxidation) \quad (18)$$

$$2O^{2-}(anodic-oxidation) = O_2 + 4e^- \quad (19)$$

$$O^{2-}(consumption) + CO_2 = CO_3^{2-} \quad (20)$$

$$v_{ET} = \frac{4Fv_{CC}}{3600 \cdot S} \quad (21)$$

F (C mol^{-1})------Faraday constant S (cm^2)------ area of cathode

As an example, Table 4 presents the calculated value of the electrolysis current density matching with the static apparent absorption rate under the selected condition based on a Ni cathode with an area of 24 cm^2. As can be seen, the process rate of MSCC-ET in $CaCO_3$-containing CaO-LiCl-KCl can be run above 239.5 mA cm^{-2} mol_{salt}^{-1}, followed by Li_2CO_3-containing Li_2O-LiCl-KCl and Li_2O-containing Li-Na-K molten carbonates, with 150.5 mA cm^{-2} mol_{salt}^{-1} and 53.6 mA cm^{-2} mol_{salt}^{-1}, respectively. Although the data are not very accurate and are obtained under specific experimental condition, it can provide some insights for the process. (1) The kinetics of CO_2 capture and reduction in $CaCO_3$-containing molten chlorides is more likely limited by electrochemical kinetics, which might be improved by applying strong electrochemical polarization within the electrochemical window; (2) The electrochemical kinetics in Li_2CO_3-containing salts is faster comparing with the absorption kinetics, the process kinetics can be improved by increasing the concentration of Li_2O and partial pressure

of CO_2 or temperature and stirring or bubbling the electrolyte. It was found in the authors' lab that the absorption rate can be accelerated by adding more Li_2O into the melt.

Summary

The effect of composition of molten salts on CO_2 absorption and electrochemical reduction process as well as the properties of the converted carbon at 450 ^oC was investigated. With the same mole amount of alkali/alkali earth oxide, CaO containing LiCl-KCl melt has the fastest absorption kinetics but the electrochemical kinetics in the melt is more sluggish and complicated. The electrochemical reduction in molten ternary carbonates is a one-step reduction process while it is a two-step process in Li_2CO_3 containing molten chlorides. For the constant current electrolysis in a two-electrode system, the cell voltage in the ternary carbonates is the lowest with highest current efficiency, demonstrating the best energy efficiency in molten carbonate. The morphology, density of structure defects, specific surface area as well as pore volume of the obtained carbon is also significantly influenced by electrolyte composition. Nano-carbon particles with a specific surface area of approximately 900 $m^2 g^{-1}$ and high I_D/I_G ratio (0.86) were obtained in the molten carbonates at a current density of 50 mA cm^{-2}. While carbon sheets with a specific area of approximately 150 $m^2 g^{-1}$ and low I_D/I_G ratio (around 0.7) were obtained in carbonate containing molten chlorides, the cation also has some effect on the property of the products. The carbon obtained in Li_2CO_3-Na_2CO_3-K_2CO_3 has a high specific capacity of more than 200 F g^{-1} due to its higher surface area and porosity. The coupling kinetics between the absorption reaction and electrochemical transformation process was further discussed based on the measured absorption and electrode kinetics. However, the process kinetics is also affected by the concentration of absorbent, temperature, pressure as well as the convention condition in the melt, which remains more investigation in future.

Acknowledgements

This work was funded by National Natural Science Foundation of China (51325102), the International Science & Technology Cooperation Program of China (2015DFA90750), the Program for Creation Team of Hubei Province (2015CFA017) and the Young-talent Chenguang Project of Wuhan City.

References

1. M. Mikkelsen, M. Jørgensen and F. C. Krebs, *Energy & Environmental Science*, 2010, **3**, 43.
2. N. MacDowell, N. Florin, A. Buchard, J. Hallett, A. Galindo, G. Jackson, C. S. Adjiman, C. K. Williams, N. Shah and P. Fennell, *Energy & Environmental Science*, 2010, **3**, 1645.
3. I. Ganesh, *Renew. Sust. Energ. Rev.*, 2014, **31**, 221-257.
4. B. Hu, C. Guild and S. L. Suib, *J. CO2 Util.*, 2013, **1**, 18-27.
5. D. T. Whipple and P. J. A. Kenis, *J. Phys. Chem. Lett.*, 2010, **1**, 3451-3458.
6. M. Aresta and A. Dibenedetto, *Dalton Trans.*, 2007, DOI: 10.1039/b700658f, 2975-2992.
7. M. Gattrell, N. Gupta and A. Co, *Journal of Electroanalytical Chemistry*, 2006, **594**, 1-19.
8. M. Alvarez-Guerra, J. Albo, E. Alvarez-Guerra and A. Irabien, *Energy & Environmental Science*, 2015, **8**, 2574-2599.
9. H. V. Ijije, R. C. Lawrence and G. Z. Chen, *RSC Adv.*, 2014, **4**, 35808-35817.
10. J. W. Fergus, *Sens. Actuator B-Chem.*, 2008, **134**, 1034-1041.
11. R. J. Bernot, E. E. Kennedy and G. A. Lamberti, *Environental Toxicology and Chemistry*, 2005, **24**, 1759-1765.
12. M. Bevilacqua, J. Filippi, H. A. Miller and F. Vizza, *Energy Technol.*, 2015, **3**, 197-210.
13. Y. Hori, H. Wakebe, T. Tsukamoto and O. Koga, *Electrochimica Acta*, 1994, **39**, 1833-1839.
14. R. Aydin, H. O. Dogan and F. Koleli, *Applied Catalysis B-Environmental*, 2013, **140**, 478-482.
15. M. J. Muldoon, S. Aki, J. L. Anderson, J. K. Dixon and J. F. Brennecke, *J. Phys. Chem. B*, 2007, **111**, 9001-9009.
16. D. M. D'Alessandro, B. Smit and J. R. Long, *Angew. Chem.-Int. Edit.*, 2010, **49**, 6058-6082.
17. T. Murakami, T. Nohira, Y. H. Ogata and Y. Ito, *Electrochem. Solid State Lett.*, 2005, **8**, E1-E3.
18. W. Xiao and D. H. Wang, *Chem. Soc. Rev.*, 2014, **43**, 3215-3228.
19. H. V. Ijije, C. Sun and G. Z. Chen, *Carbon*, 2014, **73**, 163-174.
20. B. Kaplan, H. Groult, A. Barhoun, F. Lantelme, T. Nakajima, V. Gupta, S. Komaba and N. Kumagai, *Journal of The Electrochemical Society*, 2002, **149**, D72.
21. H. Kawamura and Y. Ito, *J. Appl. Electrochem.*, 2000, **30**, 571-574.
22. S. Licht, B. H. Wang, S. Ghosh, H. Ayub, D. L. Jiang and J. Ganley, *J. Phys. Chem. Lett.*, 2010, **1**, 2363-2368.
23. H. Yin, X. Mao, D. Tang, W. Xiao, L. Xing, H. Zhu, D. Wang and D. R. Sadoway, *Energy & Environmental Science*, 2013, **6**, 1538.
24. X. Yang, L. Zhao and Y. Xiao, *Energy & Fuels*, 2013, **27**, 7645-7653.

25. D. J. Fauth, E. A. Frommell, J. S. Hoffman, R. P. Reasbeck and H. W. Pennline, *Fuel Processing Technology*, 2005, **86**, 1503-1521.
26. V. Tomkute, A. Solheim and E. Olsen, *Energy & Fuels*, 2013, **27**, 5373-5379.
27. T. Harada, F. Simeon, E. Z. Hamad and T. A. Hatton, *Chemistry of Materials*, 2015, **27**, 1943-1949.
28. H. V. Ijije, R. C. Lawrence, N. J. Siambun, S. M. Jeong, D. A. Jewell, D. Hu and G. Z. Chen, *Faraday Discuss.*, 2014, **172**, 105-116.
29. K. Le Van, H. Groult, F. Lantelme, M. Dubois, D. Avignant, A. Tressaud, S. Komaba, N. Kumagai and S. Sigrist, *Electrochimica Acta*, 2009, **54**, 4566-4573.
30. D. Chery, V. Albin, V. Lair and M. Cassir, *International Journal of Hydrogen Energy*, 2014, **39**, 12330-12339.
31. D. Chery, V. Lair and M. Cassir, *Electrochimica Acta*, 2015, **160**, 74-81.
32. S. Cavallaro and S. Freni, *J. Power Sources*, 1998, **76**, 190-196.
33. P. Greppi, B. Bosio and E. Arato, *International Journal of Hydrogen Energy*, 2009, **34**, 8664-8669.
34. K. Hemmes and M. Cassir, *Journal of Fuel Cell Science and Technology*, 2011, **8**.
35. H. Groult, B. Kaplan, S. Komaba, N. Kumagai, V. Gupta, T. Nakajima and B. Simon, *Journal of the Electrochemical Society*, 2003, **150**, G67-G75.
36. V. Kaplan, E. Wachtel, K. Gartsman, Y. Feldman and I. Lubomirsky, *Journal of the Electrochemical Society*, 2010, **157**, B552-B556.
37. D. Tang, H. Yin, X. Mao, W. Xiao and D. H. Wang, *Electrochimica Acta*, 2013, **114**, 567-573.
38. N. J. Siambun, H. Mohamed, D. Hu, D. Jewell, Y. K. Beng and G. Z. Chen, *Journal of the Electrochemical Society*, 2011, **158**, H1117-H1124.
39. K. Otake, H. Kinoshita, T. Kikuchi and R. O. Suzuki, *Electrochimica Acta*, 2013, **100**, 293-299.
40. L. Massot, P. Chamelot, F. Bouyer and P. Taxil, *Electrochimica Acta*, 2003, **48**, 465-471.
41. J. B. Ge, L. W. Hu, W. Wang, H. D. Jiao and S. Q. Jiao, *ChemElectroChem*, 2015, **2**, 224-230.
42. V. Kaplan, E. Wachtel and I. Lubomirsky, *Journal of the Electrochemical Society*, 2012, **159**, E159-E161.
43. P. Claes, D. Moyaux and D. Peeters, *Eur. J. Inorg. Chem.*, 1999, **4**, 583-588.
44. D. Peeters, D. Moyaux and P. Claes, *Eur. J. Inorg. Chem.*, 1999, **4**, 589-592.
45. L. X. Li, Z. N. Shi, B. L. Gao, J. L. Xu, X. W. Hu and Z. W. Wang, *Electrochemistry*, 2014, **82**, 1072-1077.
46. J. W. Ma, Z. Zhou, F. Zhang, C. G. Fang, Y. T. Wu, Z. B. Zhang and A. M. Li, *Environmental Science & Technology*, 2011, **45**, 10627-10633.